

# Ethene–Norbornene Copolymerization Using Homogenous Metallocene and Half-Sandwich Catalysts: Kinetics and Relationships between Catalyst Structure and Polymer Structure. 2. Comparative Study of Different Metallocene- and Half-Sandwich/Methylaluminoxane Catalysts and Analysis of the Copolymers by $^{13}\text{C}$ Nuclear Magnetic Resonance Spectroscopy

Dieter Ruchatz and Gerhard Fink\*

Max-Planck-Institut für Kohlenforschung, Kaiser-Wilhelm-Platz 1,  
45470 Mülheim an der Ruhr, Germany

Received July 15, 1997; Revised Manuscript Received April 22, 1998

**ABSTRACT:** The kinetics of ethene–norbornene copolymerizations using the metallocenes  $^i\text{Pr}[(3\text{-R-Cp})\text{-Ind}]\text{ZrCl}_2$  (with R = methyl or *tert*-butyl),  $\text{MeCH}[\text{Cp}]_2\text{ZrCl}_2$ ,  $^i\text{Pr}[(3\text{-R-Cp})\text{Flu}]\text{ZrCl}_2$  (with R = H, methyl, isopropyl, or *tert*-butyl), and  $\text{Me}_2\text{Si}[(3\text{-tert-butyl-Cp})\text{Flu}]\text{ZrCl}_2$  and half-sandwich catalysts  $\text{Me}_2\text{Si}[\text{Me}_4\text{CpN}^t\text{Bu}]\text{TiCl}_2$ ,  $\text{Me}_2\text{Si}[\text{Me}_4\text{CpN}^t\text{Bu}]\text{ZrCl}_2$ ,  $\text{Me}_2\text{Si}[\text{FluN}^t\text{Bu}]\text{ZrCl}_2$ ,  $\text{R-(+)-Me}_2\text{Si}[\text{Me}_4\text{CpNCH}(\text{CH}_3)\text{-1-naphthyl}]\text{TiCl}_2$ , and  $\text{C}_2\text{H}_4[\text{Me}_4\text{CpNMe}_2]\text{Cr}(\eta^1, \eta^1\text{-C}_4\text{H}_8)$  together with methylaluminoxane as cocatalyst, have been investigated at 70 °C in a concentrated solution of norbornene in toluene and under an ethene pressure ranging from 4 to 60 bar (58–870 psi). The ethene reaction rates were measured during the copolymerization process at various ethene concentrations and the ethene reaction orders were determined. In some cases fractional ethene reaction orders higher than 1 were found, indicating a complex mechanism. The microstructure of the copolymers were analyzed by  $^{13}\text{C}$  NMR spectroscopy. The highest norbornene contents were achieved using metallocenes with sterically less demanding ligands such as  $\text{MeCH}[\text{Cp}]_2\text{ZrCl}_2$ . Unexpectedly, low norbornene contents (<50 mol %) were achieved with the half-sandwich catalysts. Depending on the catalyst structure, the microstructure of the copolymers consists of mainly isolated norbornene units, alternating monomer sequences or short norbornene microblocks with a maximum length of two or three. Additionally, the tacticity of the norbornene microblocks could be controlled by the catalyst structure. A mechanistic model, based on chain migratory insertion, is presented to explain the different copolymer structures through nonbonding steric interactions between monomer, growing polymer chain, and ligand system. On the basis of this model, penultimate effects (Markov statistic second order) caused by the last two inserted monomer units can be assumed.

## Experimental Section

For materials and polymerizations see the preceding paper in this issue.<sup>1</sup>

**Catalysts.** All metallocenes and half-sandwich compounds were synthesized according to the literature.<sup>2–19</sup> All complex purities (> 99%) were checked by  $^1\text{H}$  NMR and MS before use.

**Polymer Characterization.** The  $^{13}\text{C}$  NMR spectra were recorded under proton broad-band decoupling at 120 °C on a Bruker AMX 300 spectrometer operating at 75 MHz. The measuring conditions are listed in Table 1.

The volume ratio of solvent:lock agent was 2:1. According to the solubility of the copolymers, 100–600 mg was dissolved in 3 mL and measured in 10 mm tubes. The spectra were related to the peak of the lock agent at 74.2 ppm. The norbornene content of the copolymers was determined by using:

mol % norbornene =

$$\frac{^{1/5}I_{\text{N(C1-C4,C7)}}}{^{1/2}(I_{\text{E,N(C5,C6)}} - ^{2/5}I_{\text{N(C1-C4,C7)}}) + ^{1/5}I_{\text{N(C1-C4,C7)}}} \quad (100)$$

where  $I_{\text{N(C1-C4,C7)}}$  = integral above the signals C1 – C4 and C7 of the norbornene (33–56 ppm) and  $I_{\text{E,N(C5,C6)}}$  = integral above the signals of ethene and C5 and C6 of the norbornene (27–32.7 ppm). The corresponding equation cited in ref 20 was found to be incorrect.

## Results and Discussion

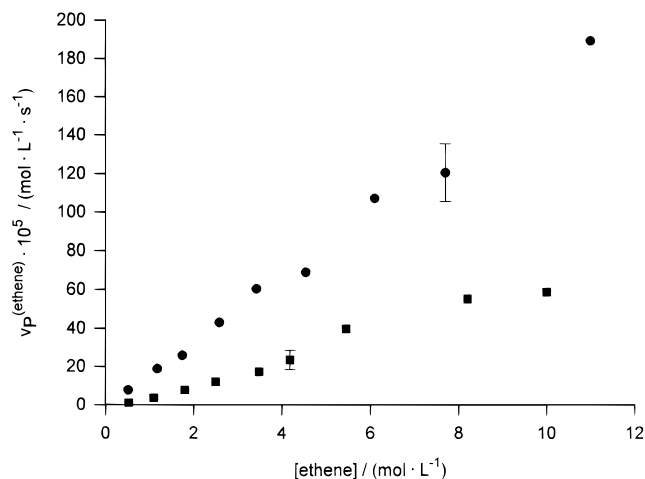
### Kinetics of the Ethene–Norbornene Copolymerization Using $^i\text{Pr}[(\text{Me-Cp})\text{Ind}]\text{ZrCl}_2/\text{Methylaluminoxane}$

Table 1. NMR Measuring Parameters

measuring frequency	75.5 Mhz
pulse angle	25°
pulse width	2.8 $\mu\text{s}$
acquisition time	1 s
relaxation time $T_1$	10 s
temperature	120 °C
solvent	1,2,4-trichlorobenzene
lock agent	1,1,2,2-tetrachloroethane- $d_2$

**minoxane and  $^i\text{Pr}[(3\text{-}^t\text{Bu-Cp})\text{Ind}]\text{ZrCl}_2/\text{Methylaluminoxane}$ .** The influence of the ethene concentration on the ethene reaction rate is shown in Figure 1. A linear dependence was found for the catalyst  $^i\text{Pr}[(3\text{-}^t\text{Bu-Cp})\text{Ind}]\text{ZrCl}_2$ , whereas a sigmoidal dependence seems to exist when the catalyst  $^i\text{Pr}[(\text{Me-Cp})\text{Ind}]\text{ZrCl}_2$  is applied. The activity of  $^i\text{Pr}[(3\text{-}^t\text{Bu-Cp})\text{Ind}]\text{ZrCl}_2$  is remarkably high, compared to the methyl-substituted catalyst type. At lower ethene concentrations, the *tert*-butyl-substituted system shows a nearly 3-fold higher ethene reaction rate than the unsubstituted  $^i\text{Pr}[\text{IndCp}]\text{ZrCl}_2$ ; at high ethene concentrations, the ethene reaction rate is 7-fold higher. At higher ethene concentrations, there is no increase in the ethene reaction rate as was already observed with  $^i\text{Pr}[\text{IndCp}]\text{ZrCl}_2$ .<sup>1</sup> For both catalysts, the ethene consumption remained constant over the entire polymerization period (maximum 70 min).

The ethene reaction orders were found to be 1 for  $^i\text{Pr}[(3\text{-}^t\text{Bu-Cp})\text{Ind}]\text{ZrCl}_2$  over the entire ethene concen-



**Figure 1.** Ethene reaction rate vs ethene concentration at 70 °C. (●)  $^i\text{Pr}[(3\text{-}^i\text{Bu-Cp})\text{Ind}]\text{ZrCl}_2$ :  $[\text{Zr}] = 2.00 \times 10^{-6} \text{ mol L}^{-1}$ ;  $[\text{Al}]/[\text{Zr}] = 4525$ ;  $[\text{norbornene}] = 7.4 \text{ mol L}^{-1}$ . (■)  $^i\text{Pr}[(\text{Me-Cp})\text{Ind}]\text{ZrCl}_2$ :  $[\text{Zr}] = 8.00 \times 10^{-6} \text{ mol L}^{-1}$ ;  $[\text{Al}]/[\text{Zr}] = 4525$ ;  $[\text{norbornene}] = 7.2 \text{ mol L}^{-1}$ .

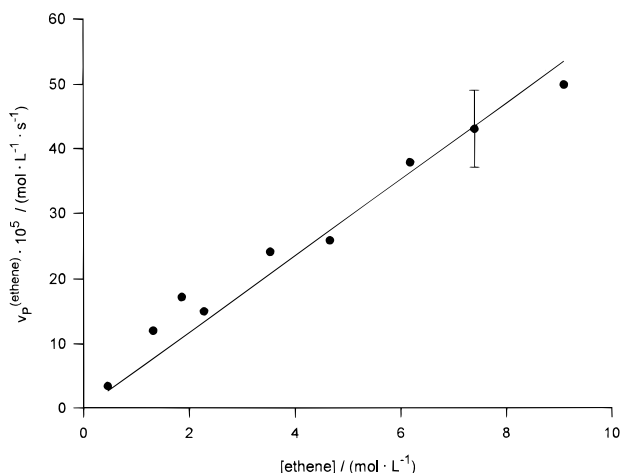


**Figure 2.** Ethene reaction rate vs ethene concentration (ethene pressure = 2–60 bar). Polymerization conditions:  $[\text{Zr}] = 8.00 \times 10^{-6} \text{ mol L}^{-1}$ ;  $[\text{Al}]/[\text{Zr}] = 4525$ ;  $[\text{norbornene}] = 7.2 \text{ mol L}^{-1}$ ;  $T = 70 \text{ }^\circ\text{C}$ .

tration range. For  $^i\text{Pr}[(\text{Me-Cp})\text{Ind}]\text{ZrCl}_2$  the ethene reaction order was determined from the first six data points in Figure 1; a fractional reaction order of 1.5 was found.

**Kinetics of the Ethene–Norbornene Copolymerization Using  $\text{MeCH}[\text{Cp}]_2\text{ZrCl}_2/\text{Methylaluminoxane}$ .** Figure 2 presents the dependence of the ethene reaction rate on the ethene concentration for  $\text{MeCH}[\text{Cp}]_2\text{ZrCl}_2/\text{methylaluminoxane}$  (MAO). A linear relationship was found over the entire ethene concentration range studied. The reaction rates are quite low and are of the same magnitude as those found previously with the  $^i\text{Pr}[(\text{Me-Cp})\text{Ind}]\text{ZrCl}_2$  catalyst. The activity of the  $\text{MeCH}[\text{Cp}]_2\text{ZrCl}_2/\text{MAO}$  catalyst was constant over the entire reaction period (30 min). The ethene reaction order was found to be 1.

**Kinetics of the Ethene–Norbornene Copolymerization Using  $^i\text{Pr}[\text{Flu-Cp}]\text{ZrCl}_2$ ,  $^i\text{Pr}[(3\text{-}^i\text{Me-Cp})\text{Flu}]\text{ZrCl}_2$ ,  $^i\text{Pr}[(3\text{-}^i\text{Prop-Cp})\text{Flu}]\text{ZrCl}_2$ ,  $^i\text{Pr}[(3\text{-}^i\text{Bu-Cp})\text{Flu}]\text{ZrCl}_2$ , and  $\text{Me}_2\text{Si}[(3\text{-}^i\text{Bu-Cp})\text{Flu}]\text{ZrCl}_2$ .** The measurement of the exact ethene reaction rates of this group of catalysts turned out to be very difficult, because the activity was extremely high after injection of the

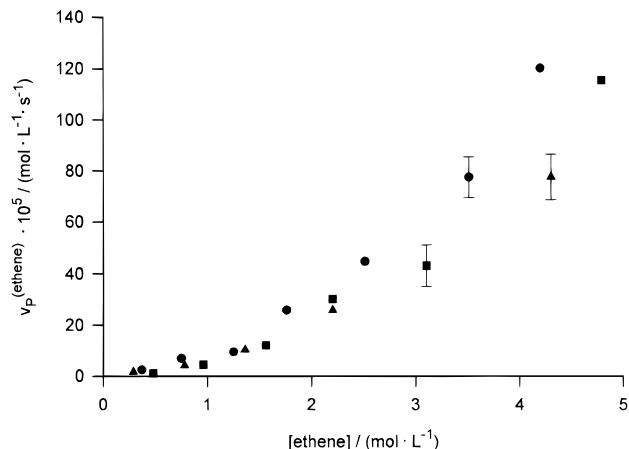


**Figure 3.** Ethene reaction rate vs ethene concentration (ethene pressure = 2–60 bar). (●)  $\text{Me}_2\text{Si}[\text{Me}_4\text{CpN}^i\text{Bu}]\text{TiCl}_2$ :  $[\text{Ti}] = 2.00 \times 10^{-6} \text{ mol L}^{-1}$ ;  $[\text{Al}]/[\text{Ti}] = 4525$ ;  $[\text{norbornene}] = 7.4 \text{ mol L}^{-1}$ . (■)  $\text{Me}_2\text{Si}[\text{Me}_4\text{CpN}^i\text{Bu}]\text{ZrCl}_2$ :  $[\text{Zr}] = 3.00 \times 10^{-5} \text{ mol L}^{-1}$ ;  $[\text{Al}]/[\text{Zr}] = 1640$ ;  $[\text{norbornene}] = 7.2 \text{ mol L}^{-1}$ . (▲)  $\text{Me}_2\text{Si}[\text{FluN}^i\text{Bu}]\text{ZrCl}_2$ :  $[\text{Zr}] = 8.00 \times 10^{-6} \text{ mol L}^{-1}$ ;  $[\text{Al}]/[\text{Zr}] = 2360$ ;  $[\text{norbornene}] = 7.3 \text{ mol L}^{-1}$ .

metallocene/MAO solution, the reaction temperature increased rapidly. After 1 or 2 min, the activity decreased to a very low but constant level, possibly due to a deactivation of the catalyst. The initial maximum ethene reaction rate could not be measured, because it was impossible to regulate the reaction temperature to a constant level before the activity loss started. An analogous kinetic behavior was found for the propene homopolymerization with some of these same catalysts.<sup>3,21</sup>

With the help of the copolymer yields, the activities were found to be 50 000–350 000 kg of copolymer/(mol of  $\text{Zr} \cdot \text{h}$ ) with the exception of the *tert*-butyl-substituted catalysts. The activity of  $^i\text{Pr}[(3\text{-}^i\text{Bu-Cp})\text{Flu}]\text{ZrCl}_2$  ranged from 3000 to 80 000 kg of copolymer/(mol of  $\text{Zr} \cdot \text{h}$ ), and the activity of  $\text{Me}_2\text{Si}[(3\text{-}^i\text{Bu-Cp})\text{Flu}]\text{ZrCl}_2$  produced values ranging between 50 and 2000 kg of copolymer/(mol of  $\text{Zr} \cdot \text{h}$ ). These are the lowest activities of all reported in this study.

**Kinetics of the Ethene–Norbornene Copolymerization Using  $\text{Me}_2\text{Si}[\text{Me}_4\text{CpN}^i\text{Bu}]\text{TiCl}_2$ ,  $\text{Me}_2\text{Si}[\text{Me}_4\text{CpN}^i\text{Bu}]\text{ZrCl}_2$ ,  $\text{Me}_2\text{Si}[\text{FluN}^i\text{Bu}]\text{ZrCl}_2$ ,  $R\text{-}(+)\text{-Me}_2\text{Si}[\text{Me}_4\text{CpNCH}(\text{CH}_3)\text{-1-Naphthyl}]\text{TiCl}_2$ , and  $\text{C}_2\text{H}_4\text{-}[\text{Me}_4\text{CpNMe}_2]\text{Cr}(\eta^1, \eta^1\text{-C}_4\text{H}_8)$ .** Within the half-sandwich catalyst group, great differences in polymerization activity were detected.  $\text{Me}_2\text{Si}[\text{Me}_4\text{CpN}^i\text{Bu}]\text{TiCl}_2$ ,  $\text{Me}_2\text{Si}[\text{Me}_4\text{CpN}^i\text{Bu}]\text{ZrCl}_2$ , and  $\text{Me}_2\text{Si}[\text{FluN}^i\text{Bu}]\text{ZrCl}_2$ , were investigated under various ethene concentrations (Figure 3). The highest activity was found for  $\text{Me}_2\text{Si}[\text{Me}_4\text{CpN}^i\text{Bu}]\text{TiCl}_2$ , whereas the Zr half-sandwich compounds were notably less active. Over the course of the copolymerization experiments with these three catalysts, the ethene consumption decreased slightly and then remained at a constant level.

The ethene reaction orders were significantly higher than 1, indicating a complex reaction mechanism. For  $\text{Me}_2\text{Si}[\text{Me}_4\text{CpN}^i\text{Bu}]\text{TiCl}_2$  the ethene reaction order was found to be 1.6; for  $\text{Me}_2\text{Si}[\text{Me}_4\text{CpN}^i\text{Bu}]\text{ZrCl}_2$ , 2.0, and for  $\text{Me}_2\text{Si}[\text{FluN}^i\text{Bu}]\text{ZrCl}_2$ , 1.5.

The results of the copolymerization experiments utilizing  $R\text{-}(+)\text{-Me}_2\text{Si}[\text{Me}_4\text{CpNCH}(\text{CH}_3)\text{-1-Naphthyl}]\text{TiCl}_2/\text{MAO}$  are listed in Table 2. The activity and temperature stability are much lower than those of  $\text{Me}_2\text{Si}[\text{Me}_4\text{CpN}^i\text{Bu}]\text{TiCl}_2$ .

**Table 2. Results of the Ethene–Norbornene Copolymerization Using R-(+)-Me<sub>2</sub>Si[Me<sub>4</sub>CpNCH(CH<sub>3</sub>)-1-naphthyl]TiCl<sub>2</sub><sup>a</sup>**

[Ti] (mol L <sup>-1</sup> )	[Al] (mol L <sup>-1</sup> )	[ethene] (mol L <sup>-1</sup> )	T (°C)	$v_p^{\text{ethene}}$ ( $\times 10^5$ mol L <sup>-1</sup> s <sup>-1</sup> )	t (min)	yield (g)	activity [kg/(mol of Ti·h)]
10 <sup>-5</sup>	0.024	1.36	50	4.3	35	2.5	1000
4.3 $\times$ 10 <sup>-5</sup>	0.03	1.36	50	10.3	44	5.3	420
4.3 $\times$ 10 <sup>-5</sup>	0.03	1.29	50	10	52	5.1	342
2 $\times$ 10 <sup>-5</sup>	0.017	1.21	70	1.7	60	1.1	137

<sup>a</sup> [Norbornene] = 7.4 mol L<sup>-1</sup>.

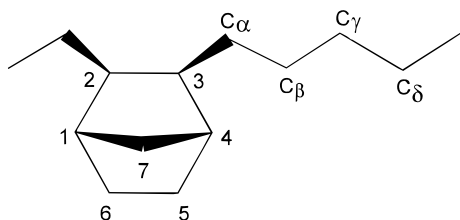


**Figure 4.** Section of an ethene–norbornene copolymer with isolated, cis-2,3-exo inserted norbornene unit.

**Table 3. Assignments of the Resonances in the <sup>13</sup>C NMR Spectrum of the Ethene–Norbornene Copolymers**

<sup>13</sup> C chemical shifts (ppm)	assignment
27.0–32.7	(C5, C6); C <sub>α</sub> , C <sub>β</sub> , C <sub>γ</sub> , C <sub>δ</sub>
29.9	(C <sub>ethene</sub> ) <sub>iso</sub> = (EEE) <sub>n</sub>
33.0–36.7	C7
37–44	C1, C4
44.5–56	C2, C3

The C<sub>2</sub>H<sub>4</sub>[Me<sub>4</sub>CpNMe<sub>2</sub>]Cr(η<sup>1</sup>,η<sup>1</sup>-C<sub>4</sub>H<sub>8</sub>)/MAO system was only tested in a few experiments, but the results indicate that this catalyst shows a relatively high activity. At a reaction temperature of 40 °C, an ethene concentration of 0.80 mol·L<sup>-1</sup> (6.0 bar) and a catalyst concentration of 5  $\times$  10<sup>-7</sup> mol L<sup>-1</sup> ([Al]/[Cr] = 16 000),  $v_p^{\text{max,ethene}}$  was calculated to be 7  $\times$  7·10<sup>-5</sup> mol L<sup>-1</sup> s<sup>-1</sup> [27 000 kg of copolymer/(mol of Cr·h)].

**<sup>13</sup>C NMR Spectroscopic Analysis of the Ethene–Norbornene Copolymers.** On the basis of the results of previous works,<sup>22–25</sup> it can be deduced that the norbornene has been cis-2,3-exo inserted during the copolymerization with all of the metallocene and half-sandwich catalysts utilized in this work. In Table 3, the assignments of the signals for the different carbon atoms are listed (for numbering of the carbon atoms, see Figure 4). Between 29 and 31 ppm, the ethene signals overlap with the C5 and C6 resonances of the norbornene. Only the resonance of the isolated CH<sub>2</sub> unit of ethene could be assigned with certainty.

According to the microstructure of the ethene–norbornene copolymers, the <sup>13</sup>C NMR spectra reveal many resonances. The reasons for this complexity of the NMR spectra include different monomer sequences, varying lengths of the norbornene microblocks, meso or racemic connection of the norbornene units, and pentad sensitivity.

The monomer sequences in Figure 5 illustrate these circumstances. The norbornene diads and triads with different carbon atom configurations at the conjunction points dramatically increase the number of anisochronic carbon atoms. Isolated meso and racemic norbornene diads, for example, have 14 resonances in the <sup>13</sup>C NMR spectrum; isolated *meso,meso*- and *rac,rac*-norbornene triads in either case have 11 different resonances; and an isolated *meso,rac*-norbornene triad has 21 possible resonances. According to the catalyst used and the

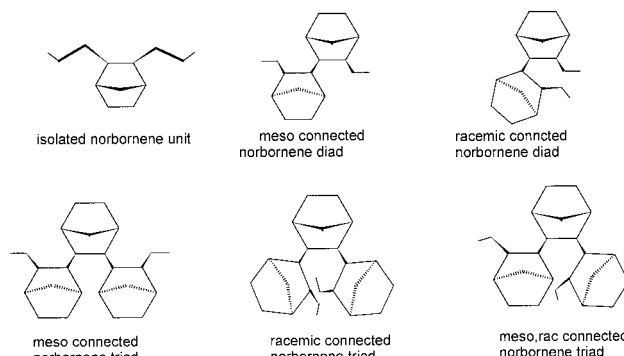


**Figure 5.** Examples of possible norbornene sequences in an ethene–norbornene copolymer.

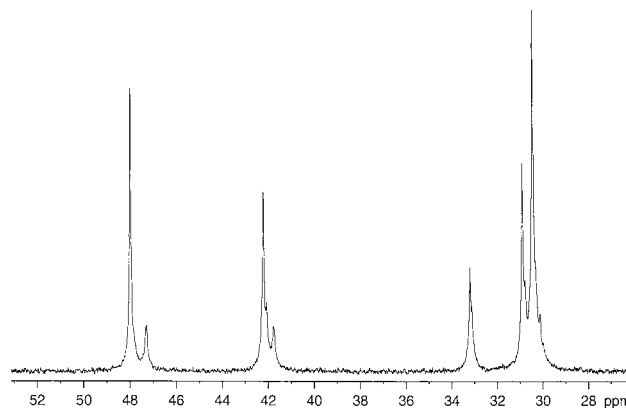


**Figure 6.** <sup>13</sup>C NMR spectrum of an ethene–norbornene copolymer with alternating monomer sequence. Catalyst: <sup>1</sup>Pr[(3-<sup>i</sup>Prop-Cp)Flu]ZrCl<sub>2</sub>; polymerization temperature = 70 °C; [norbornene]/[ethene] in solution = 6.91; norbornene content of the copolymer = 43.2 mol %.

norbornene content in the copolymer, not all of these resonances are observed simultaneously. Therefore, the specific differences in the NMR spectra measured can be investigated and interpreted with regard to the microstructure. The spectra of alternating ethene–norbornene copolymers are less complex,<sup>26</sup> which is caused by the absence of norbornene microblocks and the high symmetry of the NENEN and ENENE pentads (N = norbornene, E = ethene). In case of a perfectly alternating structure only five resonances are expected. Some of the copolymer spectra measured in the present work indicate alternating monomer sequences. These copolymers were produced by one of the following catalysts: <sup>1</sup>Pr[(3-Me-Cp)Flu]ZrCl<sub>2</sub>, <sup>1</sup>Pr[(3-<sup>i</sup>Prop-Cp)Flu]ZrCl<sub>2</sub>, <sup>1</sup>Pr[(3-<sup>i</sup>Bu-Cp)Flu]ZrCl<sub>2</sub>, Me<sub>2</sub>Si[(3-<sup>i</sup>Bu-Cp)Flu]ZrCl<sub>2</sub>, Me<sub>2</sub>Si[Me<sub>4</sub>CpN<sup>t</sup>Bu]TiCl<sub>2</sub>, Me<sub>2</sub>Si[Me<sub>4</sub>CpN<sup>t</sup>Bu]ZrCl<sub>2</sub>, R-(+)-Me<sub>2</sub>Si[Me<sub>4</sub>CpNCH(CH<sub>3</sub>)-1-naphthyl]TiCl<sub>2</sub>, or C<sub>2</sub>H<sub>4</sub>[Me<sub>4</sub>CpNMe<sub>2</sub>]Cr(η<sup>1</sup>,η<sup>1</sup>-C<sub>4</sub>H<sub>8</sub>).

Figure 6 shows the <sup>13</sup>C NMR spectrum of an ethene–norbornene copolymer with a mainly alternating structure. A comparison of a series of spectra showed that the number of resonances in the spectrum reduces to five with increasing norbornene content in the copolymer, as might be expected for an ethene–norbornene copolymer with an alternating structure. Furthermore, the presence of norbornene blocks can be excluded owing to the absence of resonances ranging below 29.9 ppm and between 35 and 41 ppm, which have been characteristic for norbornene dimers and trimers.<sup>25</sup>

This result is supported by the fact that the above-mentioned group of alternating polymerizing catalysts revealed no activity in the homopolymerization of nor-

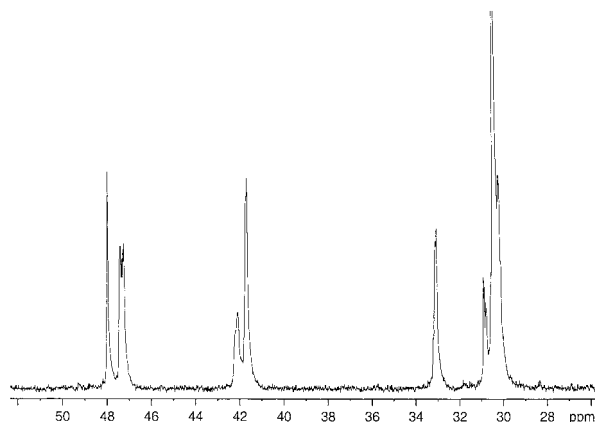


**Figure 7.**  $^{13}\text{C}$  NMR spectrum of an ethene–norbornene copolymer. Catalyst  $\text{Me}_2\text{Si}[\text{Me}_4\text{CpN}^t\text{Bu}]\text{TiCl}_2$ ; polymerization temperature =  $70^\circ\text{C}$ ; [norbornene]/[ethene] in solution = 9.8; norbornene content of the copolymer = 41.9 mol %.

bornene. In addition, the norbornene content in the copolymers, produced with these catalysts, did not exceed more than 50 mol %, as can be expected for alternating copolymers.

Are there differences in the trend of producing alternating sequences among the catalysts? The spectrum of the copolymer produced by  $\text{Me}_2\text{Si}[\text{Me}_4\text{CpN}^t\text{Bu}]\text{TiCl}_2$  answers this question (Figure 7). Differences can be observed when comparing it to the spectrum shown in Figure 6: Although both copolymers are nearly of the same norbornene content, there are more isolated norbornene units than alternating sequences in the copolymer, which was produced by the half-sandwich catalyst. This is shown by the fact that the intensity ratio  $(\text{C}2, \text{C}3)_{\text{altern}} : (\text{C}2, \text{C}3)_{\text{isol}}$  at 47.95 and 47.2 ppm is smaller than in the case of  $^1\text{Pr}[(3\text{-Me-Cp})\text{Flu}]\text{ZrCl}_2$  (see Figure 6).

The other half-sandwich catalysts tested (with the exception of  $\text{Me}_2\text{Si}[\text{FluN}^t\text{Bu}]\text{ZrCl}_2$ ) showed behavior similar to that of  $\text{Me}_2\text{Si}[\text{Me}_4\text{CpN}^t\text{Bu}]\text{TiCl}_2$ . The tendency for producing alternating sequences is less obvious than in the case of the metallocene catalysts of the  $^1\text{Pr}[(3\text{-R-Cp})\text{Flu}]\text{ZrCl}_2$  type ( $\text{R} = \text{alkyl}$ ). Therefore, these half-sandwich catalysts favor the formation of isolated norbornene units more than the alternating monomer sequences. Within the catalyst group  $\text{Me}_2\text{X}[(3\text{-R-Cp})\text{Flu}]\text{ZrCl}_2$  ( $\text{X} = \text{C or Si}$ ;  $\text{R} = \text{alkyl}$ ) there are only slight differences in the tendency for alternating monomer sequences.

The presence of attached norbornene units causes additional signals in the NMR spectrum. The analysis of a series of different copolymer spectra revealed that the following catalysts produce ethene–norbornene copolymers with norbornene microblocks:  $^1\text{Pr}[\text{IndCp}]\text{ZrCl}_2$ ,  $^1\text{Pr}[(\text{Me-Cp})\text{Ind}]\text{ZrCl}_2$ ,  $^1\text{Pr}[(3\text{-}^t\text{Bu-Cp})\text{Ind}]\text{ZrCl}_2$ ,  $\text{MeCH}[\text{Cp}]\text{ZrCl}_2$ , and  $^1\text{Pr}[\text{FluCp}]\text{ZrCl}_2$ .

The  $^1\text{Pr}[(3\text{-}^t\text{Bu-Cp})\text{Ind}]\text{ZrCl}_2$  catalyst can be regarded as being a special case: On the basis of the  $^{13}\text{C}$  NMR spectrum of the copolymer shown in Figure 8 it can be deduced that this catalyst produces norbornene microblocks with a maximum length of two. Compared to the spectra of alternating ethene–norbornene copolymers, there are additional signals to note. The three signal groups of the norbornene carbon atoms C1–C4 and C7 ranging between 32 and 50 ppm show more complex splitting, five resonances in each case. Moreover, there are two new signals detectable at 28.3 and 31.8 ppm in association, always with the same intensity, and like

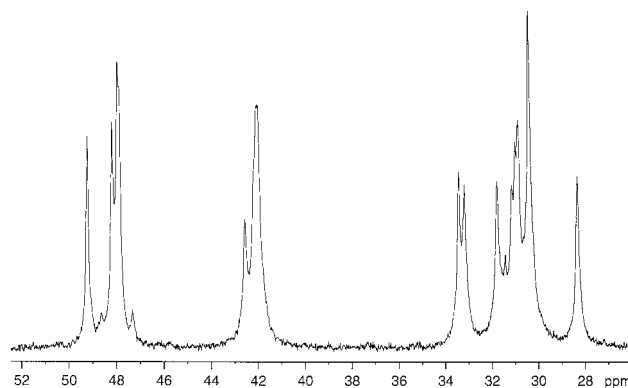


**Figure 8.**  $^{13}\text{C}$  NMR spectrum of an ethene–norbornene copolymer. Catalyst  $^1\text{Pr}[(3\text{-}^t\text{Bu-Cp})\text{Ind}]\text{ZrCl}_2$ ; polymerization temperature =  $70^\circ\text{C}$ ; [norbornene]/[ethene] in solution = 14.0; norbornene content of the copolymer = 50.7 mol %.

all other new signals, they are already observable at very low norbornene contents.

On the basis of the  $^{13}\text{C}$  NMR chemical shifts of norbornene dimers and trimers,<sup>25</sup> the resonance in the spectrum of the ethene–norbornene copolymer detected at 28.3 ppm can be assigned to C5 and C6 of the norbornene. Therefore, these resonances must be characteristic for norbornene diads in the copolymer. The signal at 31.8 ppm correlates with the norbornene diads as well, because it always appears together with the signal observed at 28.3 ppm. The reason for this signal splitting is unclear.

The characteristics of the spectrum as shown in Figure 8 do not change essentially with varying norbornene content; the signal splitting stays always the same but only the ratio of the signal intensity alters. The maximum norbornene content of the copolymers produced with  $^1\text{Pr}[(3\text{-}^t\text{Bu-Cp})\text{Ind}]\text{ZrCl}_2$  was approximately 55 mol %, whereas the activity of this catalyst in the norbornene homopolymerization remained very low. On the basis of these results it can be deduced that there are no norbornene triads or longer blocks in the copolymer. The  $^1\text{Pr}[(3\text{-}^t\text{Bu-Cp})\text{Ind}]\text{ZrCl}_2$  catalyst can be regarded as a link between the alternating polymerizing catalysts and the group of catalysts that form norbornene triads.

Copolymers with norbornene contents greater than 50 mol % could only be achieved by using the following catalysts:  $^1\text{Pr}[\text{IndCp}]\text{ZrCl}_2$ ,  $^1\text{Pr}[(\text{Me-Cp})\text{Ind}]\text{ZrCl}_2$ ,  $^1\text{Pr}[\text{FluCp}]\text{ZrCl}_2$ , and  $\text{MeCH}[\text{Cp}]\text{ZrCl}_2$ . Moreover, these catalysts showed a high activity in the homopolymerization process of norbornene.

Copolymers with more than 50 mol % norbornene must contain norbornene triads, which should be reflected in the NMR spectra. Figure 9 reveals the  $^{13}\text{C}$  NMR spectrum of an ethene–norbornene copolymer that was produced by  $^1\text{Pr}[\text{IndCp}]\text{ZrCl}_2$ . The norbornene content is 68.5 mol %. Compared to the spectra above, there are new resonances detected that range between 34 and 41.5 ppm and between 43 and 47 ppm. These additional signals in the spectrum of a copolymer holding a high norbornene content can only be explained by the presence of norbornene triads and perhaps longer norbornene microblocks. The intensity of the new signals increases with an increasing norbornene content in the copolymer. The same kind of spectrum was found for the copolymers produced by  $^1\text{Pr}[(\text{Me-Cp})\text{Ind}]\text{ZrCl}_2$ . Therefore, this catalyst too generates norbornene triads,



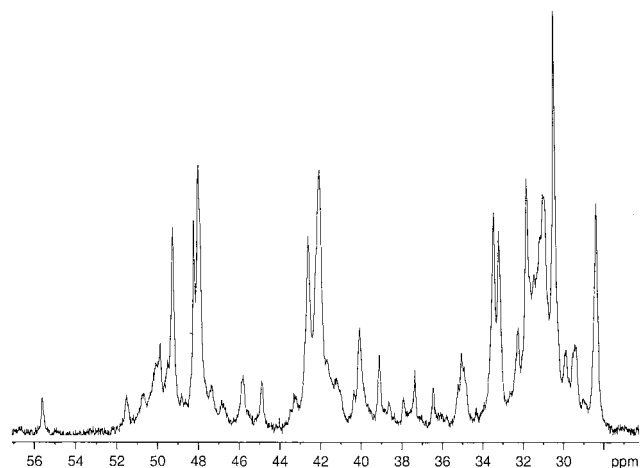


**Figure 9.**  $^{13}\text{C}$  NMR spectrum of an ethene–norbornene copolymer. Catalyst  $^i\text{Pr}[\text{IndCp}]\text{ZrCl}_2$ ; polymerization temperature =  $70^\circ\text{C}$ ; [norbornene]/[ethene] in solution = 15.1; norbornene content of the copolymer = 68.5 mol %.

but the influence of the additional methyl group at the cyclopentadienyl ligand on the microstructure is small.

The highest norbornene contents and, therefore, the longest norbornene blocks were achieved with  $\text{MeCH}[\text{Cp}]_2\text{ZrCl}_2$ . Moreover, this catalyst showed the highest activity in the norbornene homopolymerization process.

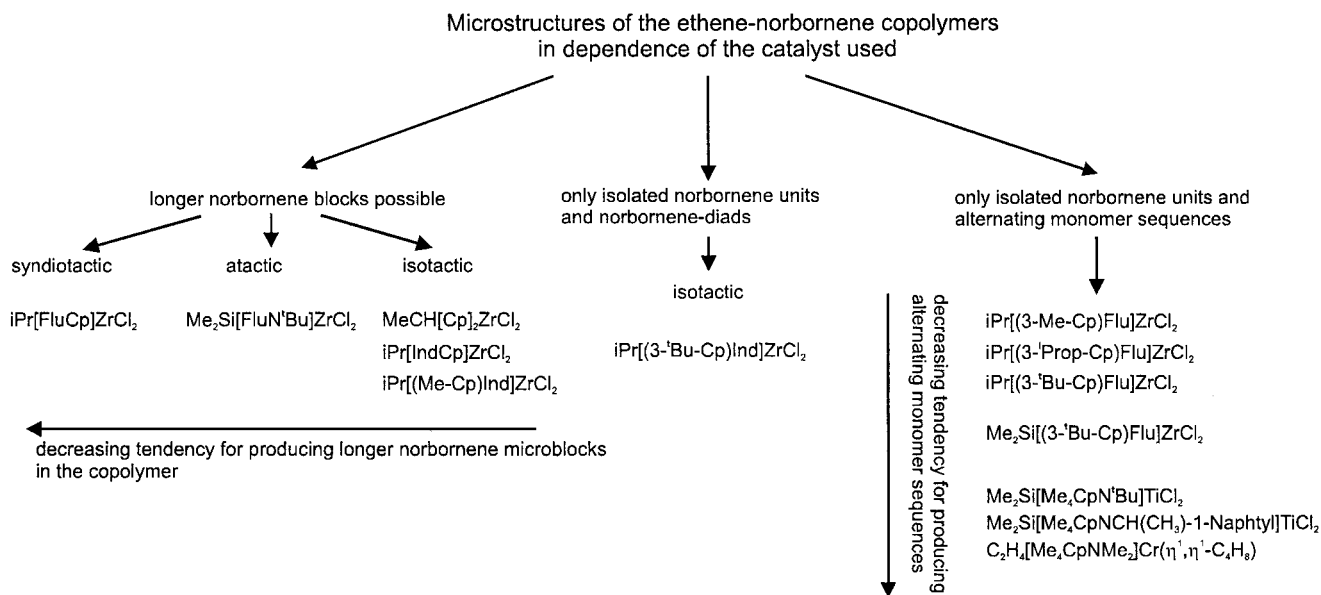
Another important aspect is the tacticity of the norbornene microblocks. As shown in Figure 5, the norbornene diads can be meso (isotactic) or racemic (syndiotactic). Arndt<sup>25</sup> disclosed that meso and racemic norbornene dimers differ in their NMR chemical shifts: In the meso compound the resonance of C5 and C6 is shifted to higher fields than found in the racemic compound. With the help of the NMR chemical shifts of the different norbornene hydrodimers and trimers, the type of connection of the norbornene units in the copolymers could be clarified.<sup>27</sup>

Figure 10 summarizes the results of the detailed  $^{13}\text{C}$  NMR analysis of the different ethene–norbornene copolymers. The catalysts can be classified into three main groups.

It is interesting that the activity observed in the norbornene homopolymerization of a catalyst can be

used as an indication of its reaction behavior during the ethene–norbornene copolymerization: Catalysts with no or little activity for the norbornene homopolymerization process produce copolymers without any norbornene microblocks (exception:  $^i\text{Pr}[(3\text{-}^i\text{Bu-Cp})\text{Ind}]\text{ZrCl}_2$ ), and catalysts with a high activity for the norbornene homopolymerization process produce copolymers with norbornene microblocks. The reason for this different reaction behavior is a result of different steric effects. The largest norbornene contents were achieved with the simplest catalysts. A sterically unhindered ligand system like the one in  $\text{MeCH}[\text{Cp}]_2\text{ZrCl}_2$  promotes the formation of longer norbornene blocks. The nonbonding interactions between the ligand, inserting norbornene, and the growing polymer chain are small when the ligand system is relatively small. Introducing a methyl group to the cyclopentadienyl ring of the ligand shows a different effect that depends on the catalyst. The differences existing between the copolymers produced by  $^i\text{Pr}[\text{IndCp}]\text{ZrCl}_2$  and  $^i\text{Pr}[(\text{Me-Cp})\text{Ind}]\text{ZrCl}_2$  are small. A more drastic effect is observed with the introduction of the methyl group in  $^i\text{Pr}[\text{FluCp}]\text{ZrCl}_2$ . The methyl group in the 3-position of the Cp ring prevents the formation of norbornene microblocks, and instead, an alternating copolymer is produced by the  $^i\text{Pr}[(3\text{-Me-Cp})\text{Flu}]\text{ZrCl}_2$  catalyst.

A good example of the influence of the growing polymer chain on the insertion process of the monomer is the  $^i\text{Pr}[(3\text{-}^i\text{Bu-Cp})\text{Ind}]\text{ZrCl}_2$  catalyst. The norbornene homopolymerization activity is very low, due to strong nonbonding interactions between the steric demands of the polynorbornene chain and the active polymerization center. However, in principle, the insertion of norbornene is possible as observed during the copolymerization with ethene. The steric interaction between the inserting norbornene and the ligand cannot be the only determining factor. Obviously, it is the structure of the polymer chain end that dictates whether an additional norbornene is inserted. After two norbornene units have been inserted, the insertion of an additional norbornene molecule is impossible, and only an ethene molecule is able to insert. The reaction behavior of the  $^i\text{Pr}[(3\text{-}^i\text{Bu-Cp})\text{Ind}]\text{ZrCl}_2$  catalyst during the norbornene homopolymerization process and ethene–norbornene



**Figure 10.** Microstructures of ethene–norbornene copolymers in dependence of the catalyst used.

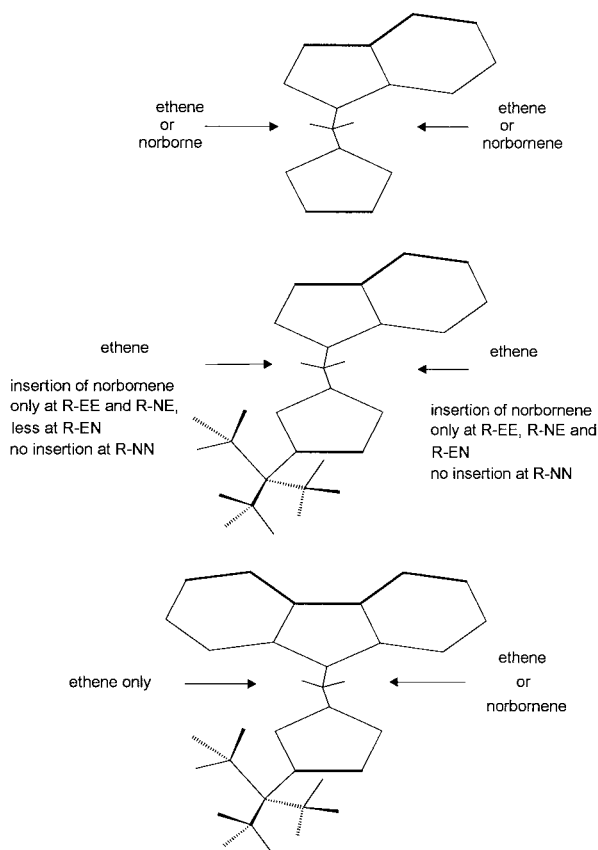


**Figure 11.** Possible insertion of ethene and norbornene at metallocenes with different coordination sites (R-XX = end sequence of the growing polymer chain; X = ethene or norbornene; metal atoms are omitted for clarity reasons).

copolymerization can, therefore, be regarded as an indication for penultimate effects (Markov statistic second order).

Figure 11 illustrates the transition from a copolymer with norbornene microblocks to an alternating copolymer on the basis of the chain migratory insertion (alternating insertion). The influence of the substituent in the 3-position on the Cp ligand plays the decisive role. The insertion proceeds via migration of the growing polymer chain to the site where the olefin is coordinated. Consequently, the next insertion step begins at interchanged coordination sites of the polymer chain and coordinated olefin. The coordination takes place in an alternating manner from one side of the metallocene to the other.

The growing polymer chain and the coordinated norbornene have enough room to evade each other. Conforming to these circumstances, the norbornene insertion is not favored by one of the two possible conformations and the insertion of the norbornene proceeds from both coordination sites, which enables the formation of longer norbornene microblocks in the copolymer and during the homopolymerization process of norbornene. The mainly isotactic structure of the norbornene blocks in the copolymer shows that it is not the symmetry of the metallocene which is decisive but the relative energy differences between the possible conformation minima with *re*- or *si*-coordinated olefin as shown by Fink et al. in the case of propene homopolymerization.<sup>28,29</sup>

A different situation occurs when a *tert*-butyl group is introduced: Ethene–norbornene copolymers that are

produced by  $^i\text{Pr}[(3\text{-}^i\text{Bu-Cp})\text{Ind}]\text{ZrCl}_2$  contain *meso*-connected norbornene microblocks with a maximum length of two and the norbornene homopolymerization activity is nearly zero. The insertion of norbornene is restricted on both sides of the metallocene, due to the larger sterical demands of the *tert*-butyl group. But the restriction is not the same for both sides of the catalyst, as shown in Figure 11: The norbornene insertion is not possible at the growing polymer chain with the ending sequence R–NN (R = polymer chain, N = norbornene unit at the end of the chain) and therefore  $k_{\text{NNN}} = 0$ . At the sterically less hindered coordination site, the norbornene insertion can proceed at the chain endings with the sequence R–EE, R–NE, or R–EN (E = ethene unit). From the sterically more hindered coordination site, which is directly influenced by the *tert*-butyl group, only at the chain ending sequences R–EE and R–NE can the norbornene insertion proceed. The norbornene insertion at the sequence R–EN from the sterically more hindered coordination site cannot play an important role, because if so a copolymer with a pseudoalternating structure such as –ENNENNENNENNENN– would be formed in an extreme case. The occurrence of this monomer sequence can be excluded, because such a copolymer would contain up to 67 mol % norbornene, but in the experiment the content does not exceed much more than 50 mol %. Furthermore, an ethene–norbornene copolymer with the above-mentioned pseudoalternating sequence would cause a simpler NMR spectrum. But perhaps it is possible to produce a pseudoalternating copolymer, if the *tert*-butyl group could be exchanged for another alkyl group like, for example, ethyl or isopropyl. The observation of *meso*-norbornene diads (isotactic structure) is in agreement with the results of the propene homopolymerization, where a mainly isotactic polypropene was produced with  $^i\text{Pr}[(3\text{-}^i\text{Bu-Cp})\text{Ind}]\text{ZrCl}_2$ .<sup>3</sup>

An extreme case occurs when catalysts of the  $\text{Me}_2\text{X}[(3\text{-R-Cp})\text{Flu}]\text{ZrCl}_2$  type (with R = methyl, isopropyl, or *tert*-butyl and X = C or Si) are used, as demonstrated for R = *tert*-butyl, which is shown at the bottom of Figure 11. The sterically more hindered coordination site is now totally blocked off by the *tert*-butyl group and half of the fluorenyl ligand. Only ethene can be inserted from this side. Both monomers can be inserted from the less hindered side. In accordance with this explanation, a copolymer with an alternating structure can be formed through this group of catalysts.

The reaction behavior of the half-sandwich catalysts with amido ligands was unexpected, because it is said that these types of catalysts possess a sterically less demanding ligand system and, therefore, have less difficulty inserting larger monomers.<sup>30</sup> The present work shows that these results cannot be generalized, especially in the case of cycloolefins. The norbornene contents in the copolymer that were achieved by using different half-sandwich catalysts are comparable to those from the metallocene such as  $^i\text{Pr}[(3\text{-}^i\text{Bu-Cp})\text{Flu}]\text{ZrCl}_2$  and are, therefore, relatively low. In general, the half-sandwich catalysts tested produced no copolymers with norbornene microblocks—a result that was to be expected on grounds of the nonexistent norbornene homopolymerization activity (with the exception of  $\text{Me}_2\text{-Si}[\text{FluN}^i\text{Bu}]\text{ZrCl}_2$ ).

## References and Notes

- (1) Ruchatz, D.; Fink, G. *Macromolecules* **1998**, *31*, 4669–4673 (first of four papers in this issue).

- (2) Spaleck, W.; Antberg, M.; Dolle, V.; Klein, R.; Rohrmann, J.; Winter, A. *New J. Chem.* **1990**, *14*, 499.
- (3) R. Kleinschmidt, Diplomarbeit, Universität Düsseldorf, Germany, 1996.
- (4) Herrmann, G. S.; Alt, H. G.; Rausch, M. D. *J. Organomet. Chem.* **1991**, *401*, C5.
- (5) Ewen, J. A.; Jones, R. L.; Razavi, A.; Ferrara, J. D. *J. Am. Chem. Soc.* **1988**, *110*, 6255.
- (6) Dolle, V.; Rohrmann, J.; Winter, A.; Antberg, M.; Klein, R. European Patent EP 399 347, 1989.
- (7) Antberg, M.; Dolle, V.; Klein, R.; Rohrmann, J.; Spaleck, W.; Winter, A. In *Catalytic Olefin Polymerization*; Soga, K.; Keii, T., Eds.; Kodansha: Tokyo, 1990.
- (8) Ewen, J. A. European Patent EP 423 101, 1989.
- (9) Ewen, J. A.; Elder, M. J. European Patent EP 537 130, 1993.
- (10) Ewen, J. A.; et al. *Macromol. Chem. Macromol. Symp.* **1991**, *48/49*, 253.
- (11) Ewen, J. A.; Elder, M. J. European Patent EP 537 130, 1993.
- (12) Ewen, J. A.; Elder, M. J. In *Ziegler Catalysts, Recent Scientific Innovations and Technological Improvements*; Fink, G.; Mülhaupt, R.; Brintzinger, H.-H., Eds.; Springer: Berlin Heidelberg New York, 1995.
- (13) Stevens, J. C.; Timmers, F. J.; Wilson, D. R.; Schmidt, G. F.; Nicklas, P. N.; Rosen, R. K.; Knight, G. W.; Lai, S., EP 416815, EXXON, 1990.
- (14) Canich, J. A. M. (Exxon). European Patent EP 420 436, 1990.
- (15) Canich, J. A. M. U.S. Patent 5026798, 1991.
- (16) U.S. Patent 5055438, 1991.
- (17) Devore, D. D. (Dow). European Patent EP 514 828, 1992.
- (18) van der Leek, Y. Dissertation, Universität Düsseldorf, Germany, 1996.
- (19) Verhovnik, G. Dissertation, Universität Bochum, Germany, 1996.
- (20) Noll, A. Dissertation, Universität Hamburg, Germany, 1993.
- (21) Herfert, N. Dissertation, Universität Düsseldorf, Germany, 1992.
- (22) Kaminsky, W.; Bark, A.; Däke, I. *Polymerization of Cyclic Olefins with Homogeneous Catalysts*. In *Catalytic Olefin Polymerization*; Soga, K.; Keii, T., Eds.; Kodansha: Tokyo, 1990.
- (23) Kaminsky, W.; Bark, A.; Arndt, M. *Makromol. Chem., Macromol. Symp.* **1991**, *47*, 83–93.
- (24) Bark, A. Dissertation, Universität Hamburg, Germany, 1990.
- (25) Arndt, M. Dissertation, Universität Hamburg, Germany, 1994.
- (26) Cherdron, H.; Brekner, M.-J.; Osan, F. *Angew. Makromol. Chem.* **1994**, *223*, 121.
- (27) Ruchatz, D. Dissertation, Universität Düsseldorf, Germany, 1997.
- (28) Montag, P.; van der Leek, Y.; Angermund, K.; Fink, G. *J. Organomet. Chem.* **1995**, *497*, 201.
- (29) van der Leek, Y.; Angermund, K.; Reffke, M.; Kleinschmidt, R.; Goretzki, R.; Fink, G. *Chem. Eur. J.* **1997**, *3*, 585.
- (30) Brintzinger, H.-H.; Fischer, D.; Mülhaupt, R.; Rieger, B.; Waymouth, R. *Angew. Chem.* **1995**, *107*, 1255.

MA971042J